Supporting Information

Potential screening of oral squamous cell carcinoma using microRNA geno-assay by electrochemical sensing: A new platform in biosensor technology

Hamed Bahari [a,b] , Mohammad Hasanzadeh [a,*], Soodabeh Davaran [b**], Farzin Ahmadpour [c], Fereshteh Kohansal [d], Nasrin Shadjou [e]

[a] Pharmaceutical Analysis Research Center, Pharmaceutical Sciences Institute, Tabriz University of Medical Science, Tabriz, Iran.
[b] Research Center for Pharmaceutical Nanotechnology, Pharmaceutical Sciences Institute, Tabriz University of Medical Science, Tabriz, Iran.
[c] Department of Medical Nanotechnology, Faculty of Advanced Medical Sciences, Tabriz University of Medical Sciences, Tabriz, 516661-4733, Iran.
[d] Department of Oral and Maxillofacial Surgery, Dentistry Faculty, Tabriz University of Medical Sciences, Tabriz, Iran
[e] Drug Applied Research Center, Pharmaceutical Sciences Institute, Tabriz University of Medical Science, Tabriz, Iran.
[f] Department of Nanotechnology, Faculty of Chemistry, Urmia University, Urmia, Iran

Corresponding Authors:
* **Mohammad Hasanzadeh**; Pharmaceutical Analysis Research Center, Tabriz University of Medical Sciences, Tabriz, Iran.
(*) hasanzadehm@tbzmed.ac.ir
** **Soodabeh Davaran**; Department of Medical Nanotechnology, Faculty of Advanced Medical Sciences, Tabriz University of Medical Sciences, Tabriz, 516661-4733, Iran.
(**) davaran@tbzmed.ac.ir

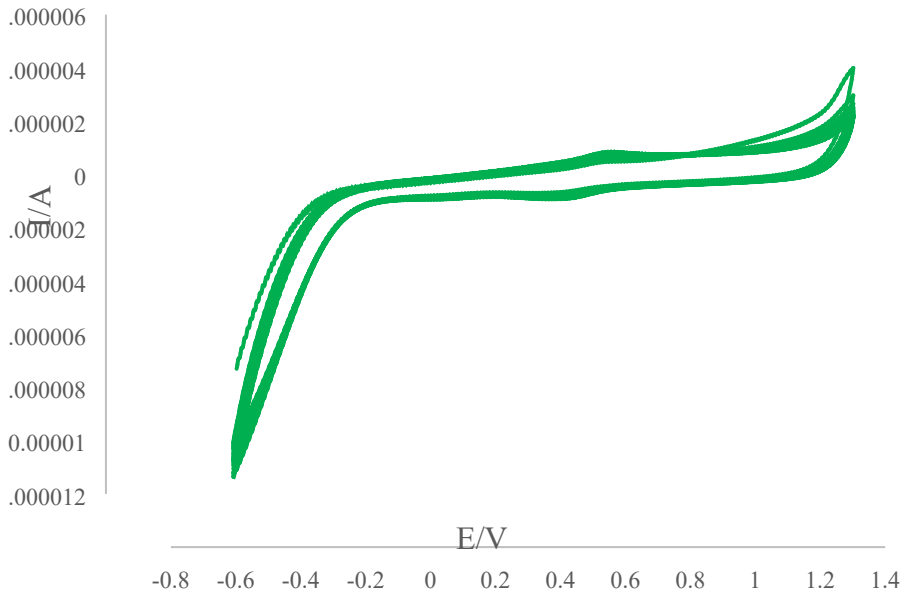

Fig. S1: CVs of GCE in the present of CS solution (0.005 gr in 0.1 M acetic acid) in the scan rate = 100 mV/s; number of cycles = 20.

A)

B)

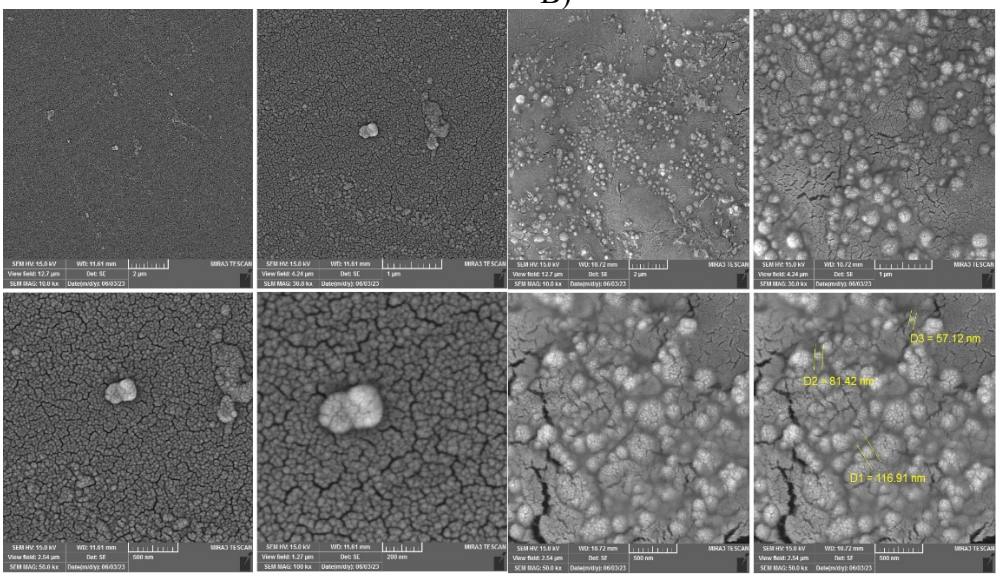
D3 = 57.12 nm
D2 = 81.42 nm
D1 = 116.91 nm

C)

D)

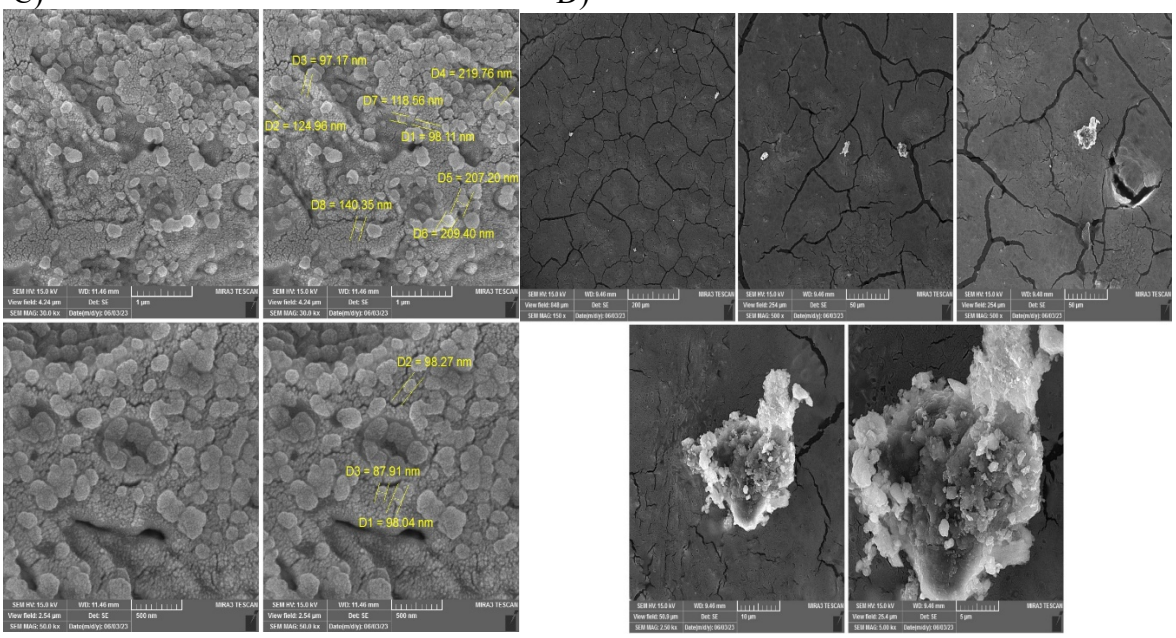
D3 = 97.17 nm
D4 = 219.76 nm
D7 = 116.56 nm
D2 = 124.96 nm
D1 = 98.11 nm
D5 = 207.20 nm
D8 = 140.35 nm
D6 = 209.40 nm
D2 = 98.27 nm
D3 = 87.91 nm
D1 = 98.04 nm

E)

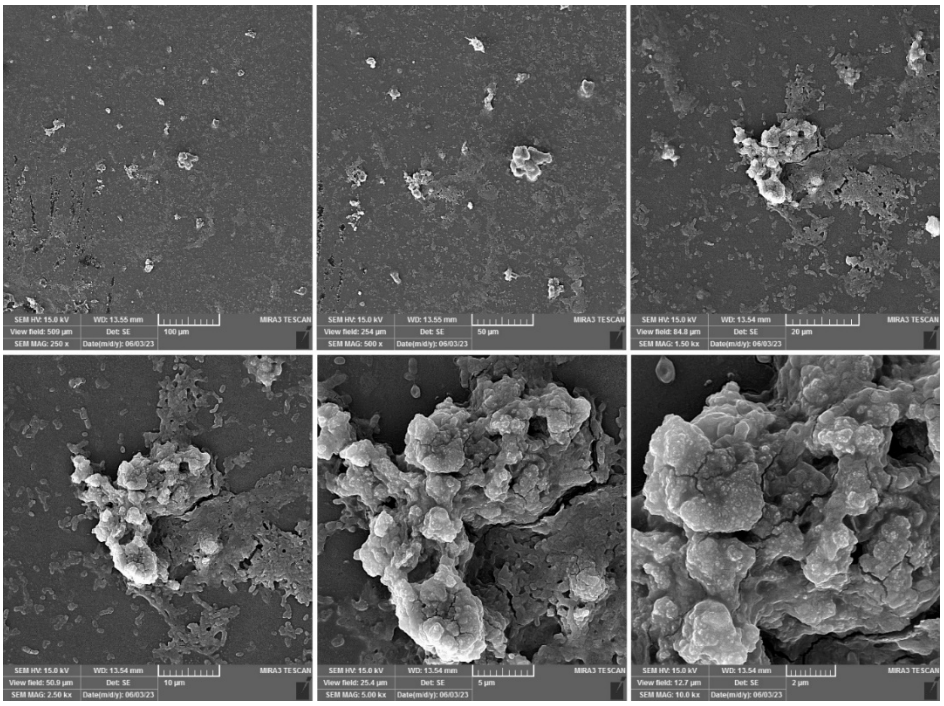

Fig. S2: FE-SEM images of **A)** P(CS), **B)** P(CS)-KCC-1-nPr-NH-Arg, **C)** P(CS) KCC-1-nPr-NH-Arg-AgNPs, **D)** P(CS)-KCC-1-nPr-NH-Arg-AgNPs-probeDNA, **E)** P(CS)-KCC-1-nPr-NH-Arg-AgNPs-probeDNA-BSA-MicroRNA-423-5p in different magnifications.

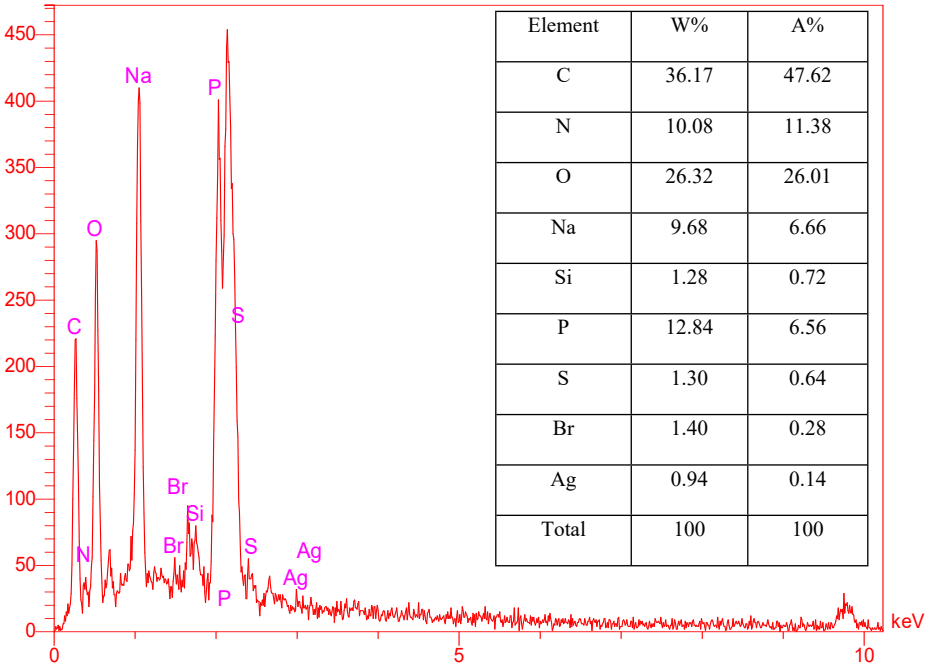

Element	W%	A%
C	36.17	47.62
N	10.08	11.38
O	26.32	26.01
Na	9.68	6.66
Si	1.28	0.72
P	12.84	6.56
S	1.30	0.64
Br	1.40	0.28
Ag	0.94	0.14
Total	100	100

Fig. S3. EDS spectra of fabricated genosensor.

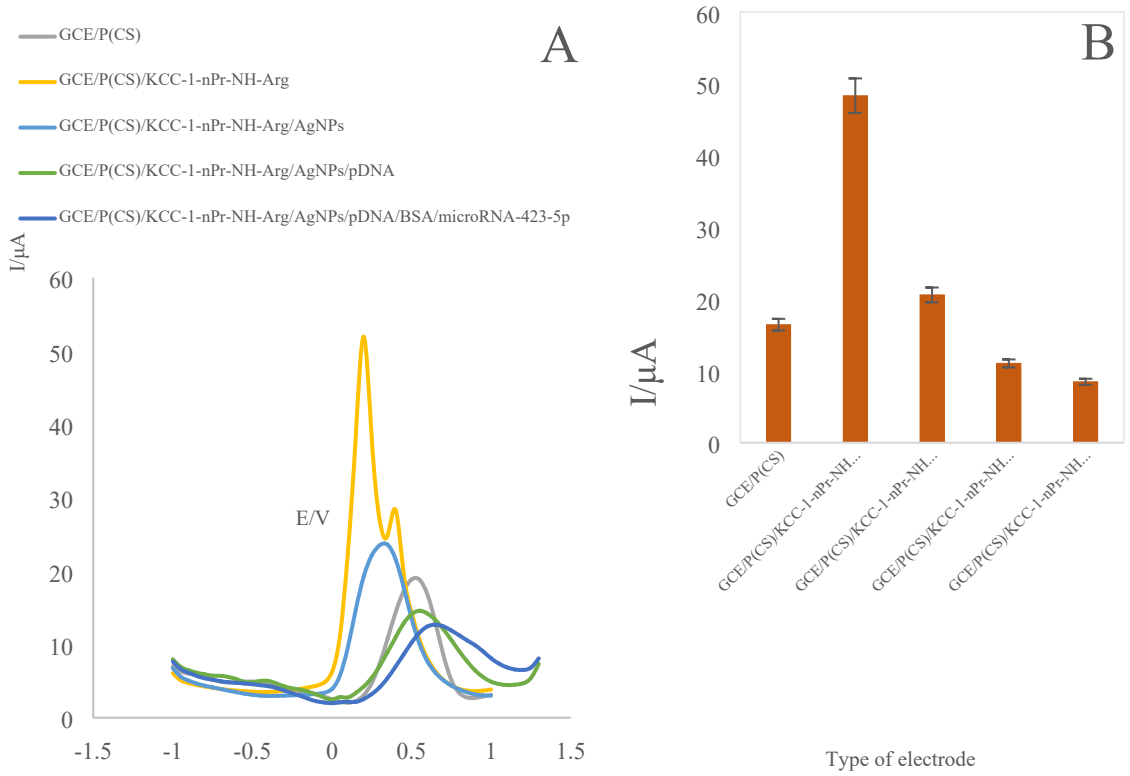

Fig. S4. A) DPVs of bare GCE, P(CS)-modified GCE, P(CS)-KCC-1-nPr-NH-Arg-modified GCE, P(CS)-KCC-1-nPr-NH-Arg-AgNPs-modified GCE, P(CS)-KCC-1-nPr-NH-Arg-AgNPs-probeDNA-modified GCE, P(CS)-KCC-1-nPr-NH-Arg-AgNPs-probeDNA-BSA-microRNA-modified GCE in 0.01 M $Fe(CN)_6^{-3/-4}$ and 0.01 M KCl as the supporting electrolyte with a sweep rate of 100 mV/s. **B)** Bar-graph of changes in peak current at different stages of genosensor fabrication.

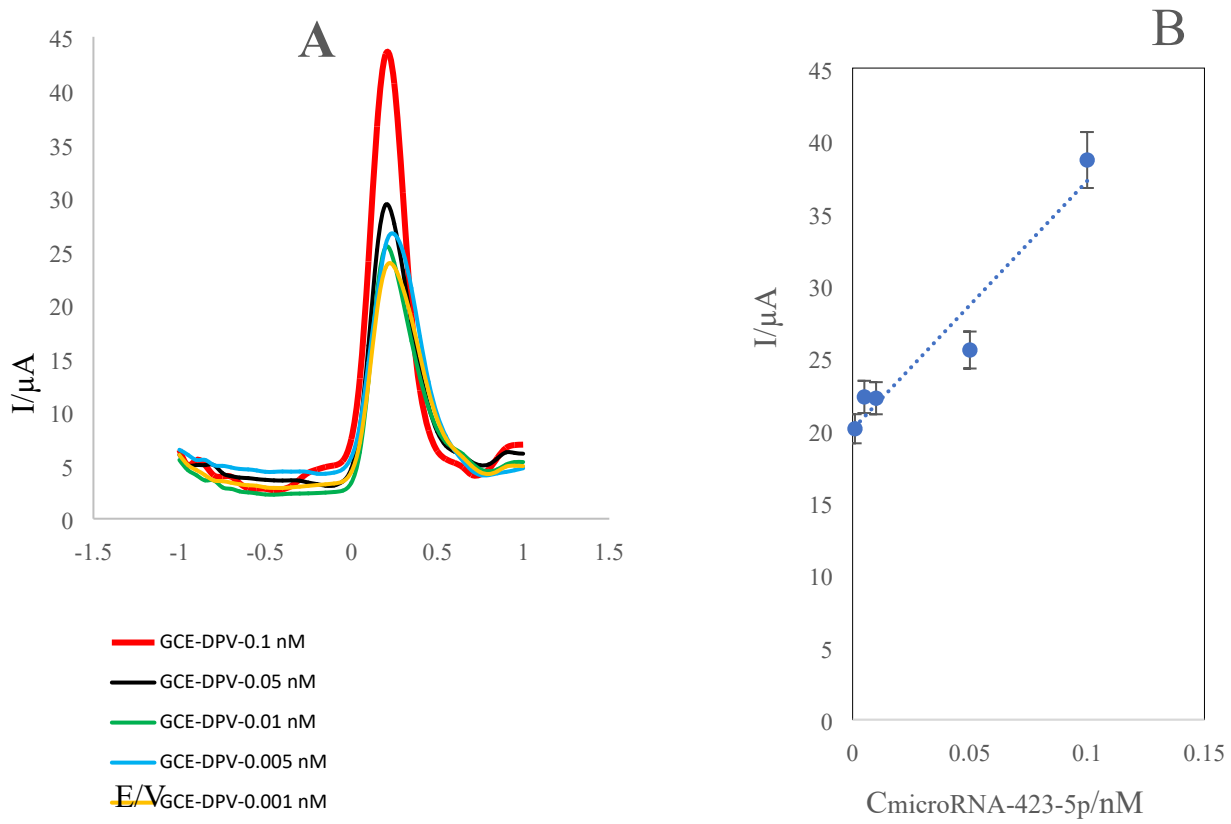

Fig. S5: A) DPVs of the genosensor in different concentrations of microRNA-423-5p: 0.1, ,0.05, 0.01, 0.005, 0.001 nM with treated human plasma sample in the present of 0.01 M $Fe(CN)_6^{-3/-4}$ and 0.01 M KCl as the supporting electrolyte **B)** Calibration curve against the concentration value microRNA-423-5p.

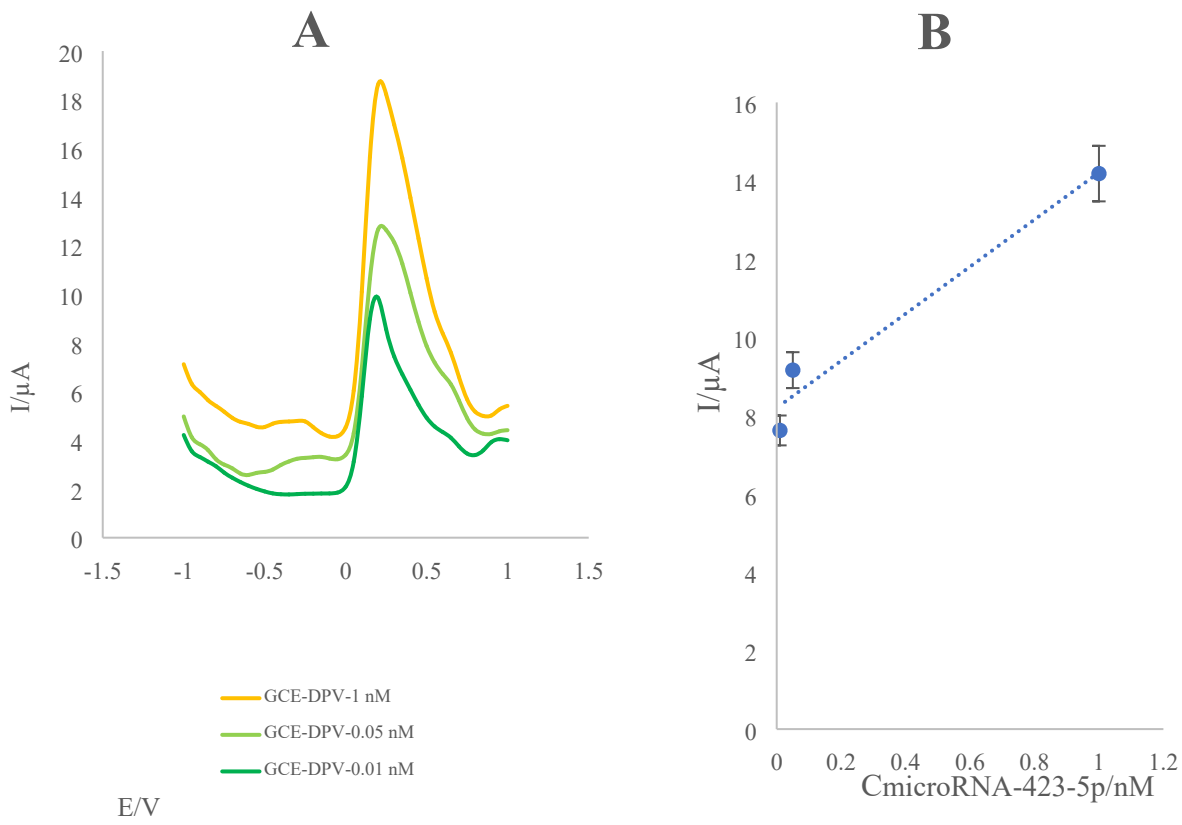

Fig. S6: **A)** DPVs of the constructed genosensor in the present of different concentrations of microRNA-423-5p: 0.01,0.05, 1 nM with healthy human saliva samples in 0.01 M $Fe(CN)_6^{-3/-4}$ and 0.01 M KCl as the supporting electrolyte **B)** Calibration curve of biosensor versus the amount of microRNA-423-5p.

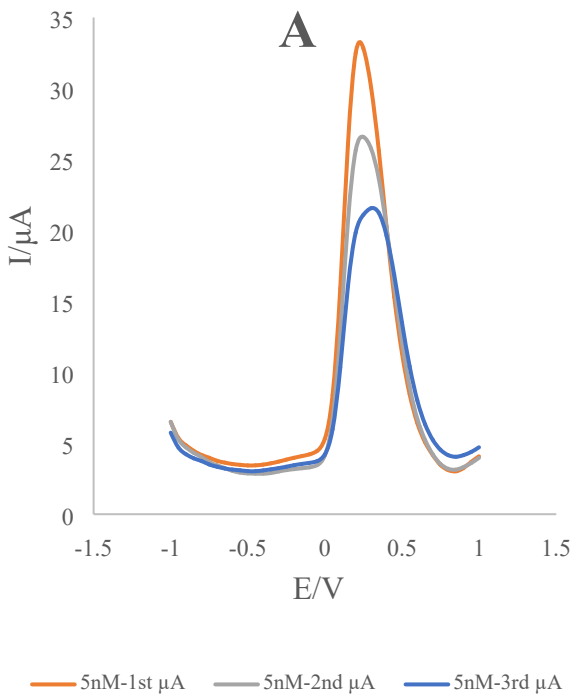
A
I/μA
E/V
5nM-1st μA
5nM-2nd μA
5nM-3rd μA

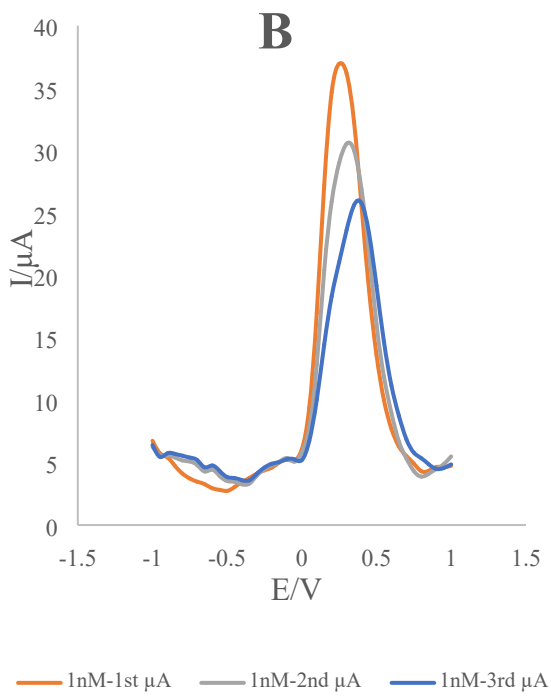
B
I/μA
E/V
1nM-1st μA
1nM-2nd μA
1nM-3rd μA

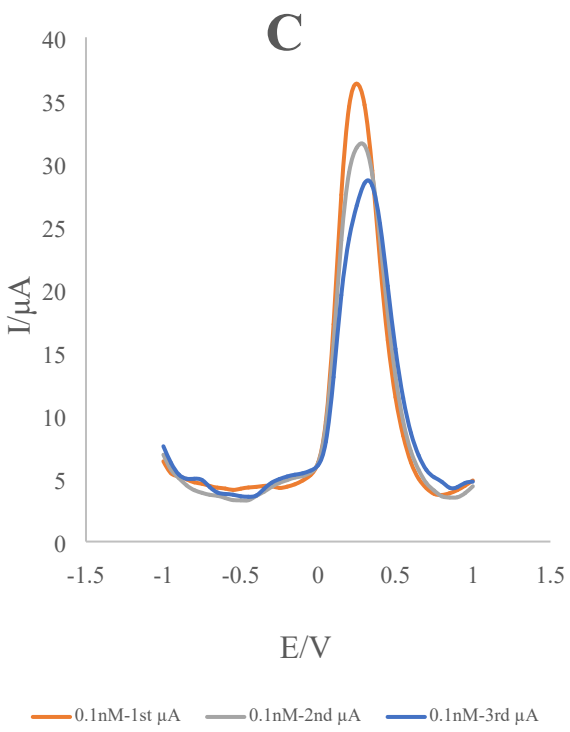
C
I/μA
E/V
0.1nM-1st μA
0.1nM-2nd μA
0.1nM-3rd μA

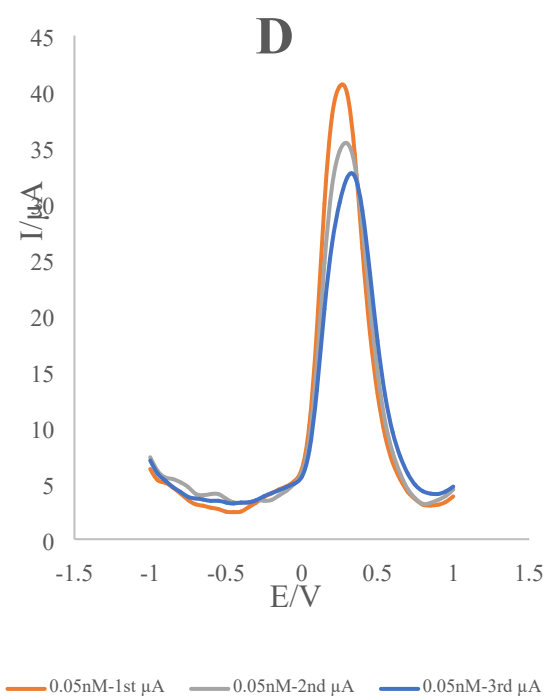
D
I/μA
E/V
0.05nM-1st μA
0.05nM-2nd μA
0.05nM-3rd μA

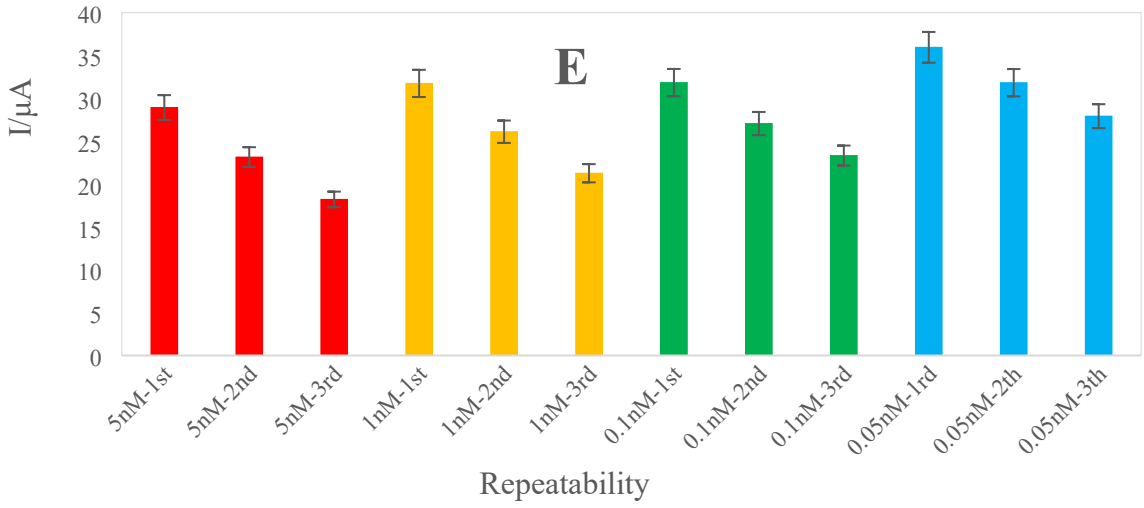

Fig. S7: A, B, C, D) DPVs of genosensor recorded for repeatability of 5, 1, 0.1 and 0.05 nM concentrations in 0.01 M $Fe(CN)_6^{-3/-4}$ and 0.01 M KCL as the supporting electrolyte B) Histogram of peak current *vs* different concentrations of microRNA-423-5P sequences in 3 repetitions.

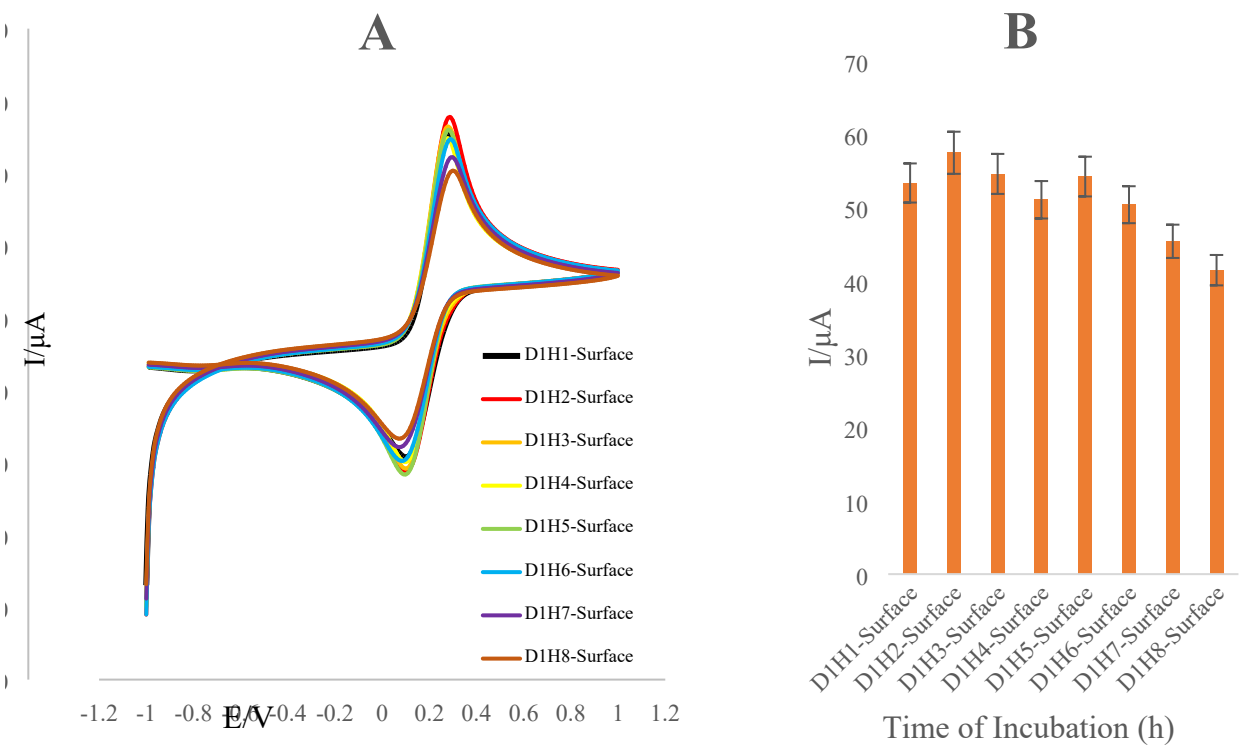

Fig. S8: A) CVs of P(β-CD)/KCC-1-nPr-NH-Arg-modified GCE in the potential range of -1 to 1 and sweep rate of 0.1 V/s in the presence of 0.01 M $Fe(CN)_6^{-3/-4}$ and 0.01 M KCL as the supporting electrolyte in different time of incubation. **B)** Histogram of peak current *vs* time of incubation.

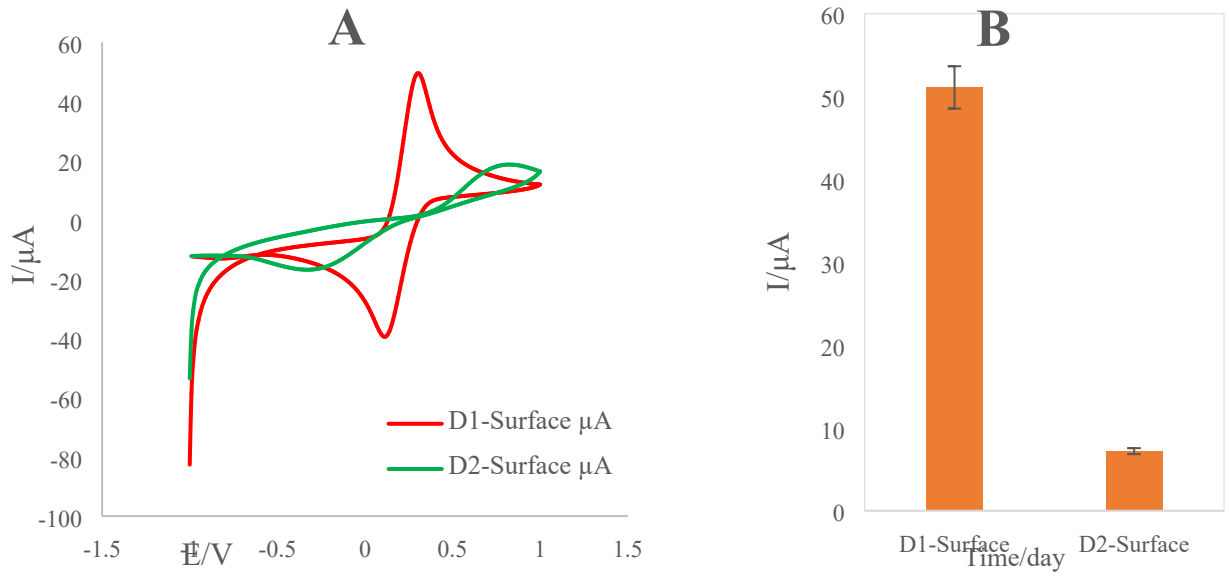

Fig. S9: A) CVs of P(β-CD)/KCC-1-nPr-NH-Arg-modified GCE in the potential range of -1 to 1 and sweep rate of 0.1 V/s in the presence of 0.01 M $Fe(CN)_6^{-3/-4}$ and 0.01 M KCL as the supporting electrolyte in different time of incubation. **B)** Histogram of peak current *vs* period time of detection.

Kinetic Study

The scan rate plays a crucial role in redox analysis, as it allows for the examination of the electrochemical behavior of various analytes on the electrode surface. By studying the connection between the scan rate and peak currents, we may get insights into the electrochemical reaction process. An investigation was conducted on the redox properties of the GCE/P(CS)/KCC-1-nPr-NH-Arg/AgNPs electrode utilizing $Fe(CN)_6^{-3/-4}$ /KCl. The CV of the electrode was recorded at various sweep rates (2, 5, 10, 20, 30, 40, 50, 60, 70, 90, 100, and 150 mV/s).

According to the obtained CV graph (Figure S10A), an increase in scan rate resulted in a progressive broadening of the voltammogram and a significant alteration in the anodic peak current. Electrons have a high probability of transferring at the electrode contact, leading to an increase in the peak current. The pace of this process decelerates as the scan speeds are decreased. Also, Figure S10B demonstrates that there is a direct correlation between anodic/cathodic peak currents *versus* the sweep rates (2 to 150 $mV.s^{-1}$).

The relationship between I_p *vs* $v^{0.5}$, as well as the relationship between I_p vs Ln *v*, are being examined by CV technique. Figure S10(C and D) illustrate the patterns seen in the oxidation peak. In the absence of any kinetic complications in both reversible and irreversible systems, the values of I_p (peak current) and $v^{0.5}$ (half-wave potential) are directly related and meet at the origin of the figure. Figure S10C clearly illustrates the linear relationship between the I_{pa} and $v^{0.5}$ curve, exhibiting a high coefficient of determination (R^2 = 0.9937) and intersecting the origin. The connection is expressed by the following equation:

$$I_{pa}\ (\mu A) = 175.23\ v^{0.5}\ (V/s)^{0.5} - 3.3323\ (R^2 = 0.9937)$$

It can be inferred that electron transport kinetics are governed by diffusion due to the root connection between the variables.

In the selected sweep rate range of 2 to 150 mV s^{-1}, the dependence between ln I_{pa} and ln v (Figure S10D) is linear. This may be understood by using the following equation:

$$\text{Ln } I_{pa} \text{ (}\mu\text{A)} = 4.1564e^{0.5461} \text{ Ln } v \text{ (mV/s)} + 117.96 \text{ (}R^2 = 0.9955\text{)}$$

It displays diffusion-control of the electrode process and has a slope of 0.5. It is anticipated that the slopes of diffusion-controlled systems will be close to 0.5 and those of adsorption-controlled systems would be close to 1.

Figure S10E shows the link between sweep rate and E_{pa} (anodic peak potential). The sweep rate and E_{pa} of irreversible electrochemical processes are independent of one another. Given that raising the sweep rate causes E_{pa} to increase, this shows that the electron transfer in these events is irreversible.

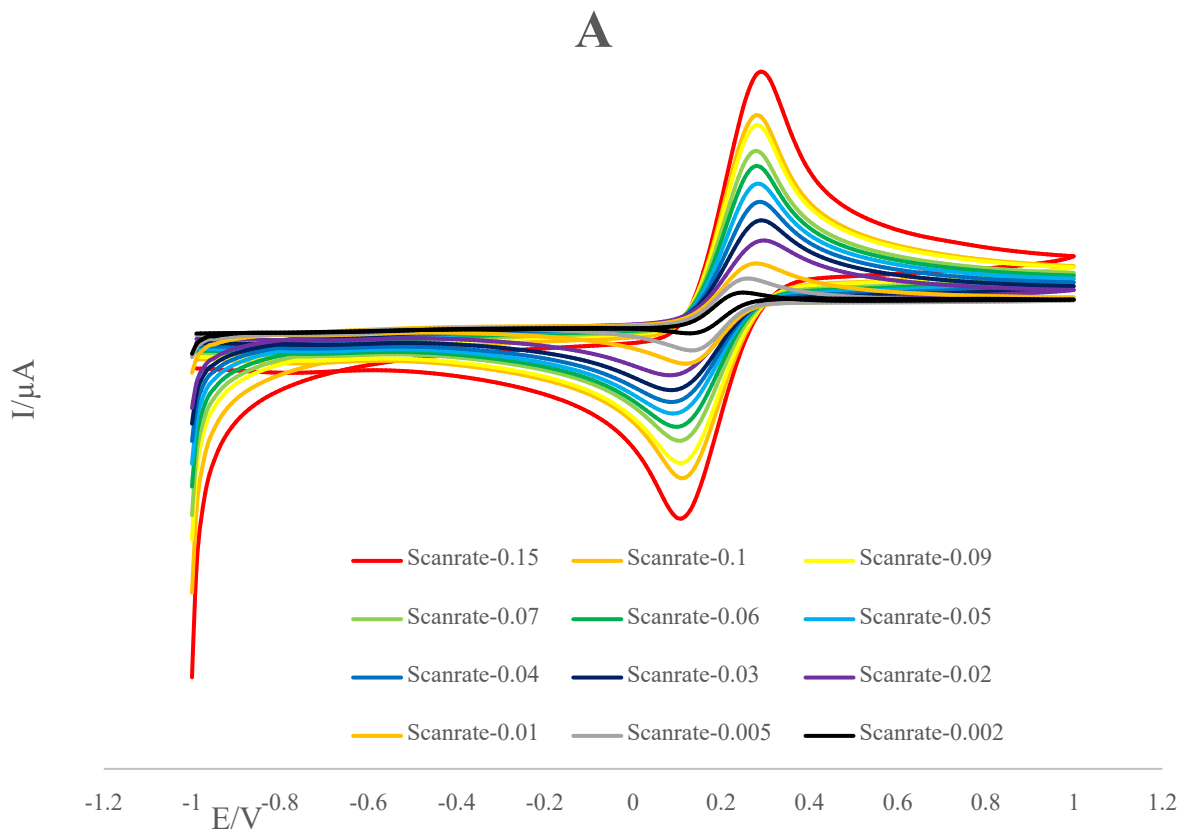
A
I/μA
Scanrate-0.15
Scanrate-0.1
Scanrate-0.09
Scanrate-0.07
Scanrate-0.06
Scanrate-0.05
Scanrate-0.04
Scanrate-0.03
Scanrate-0.02
Scanrate-0.01
Scanrate-0.005
Scanrate-0.002
-1.2
-1
E/V
-0.8
-0.6
-0.4
-0.2
0
0.2
0.4
0.6
0.8
1
1.2

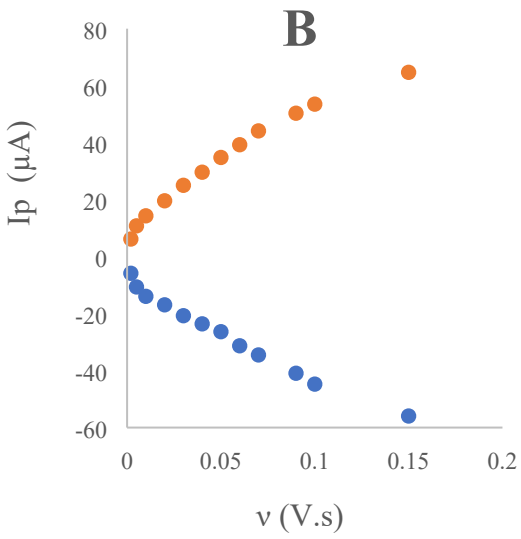
B
Ip (μA)
80
60
40
20
0
-20
-40
-60
0
0.05
0.1
0.15
0.2
ν (V.s)

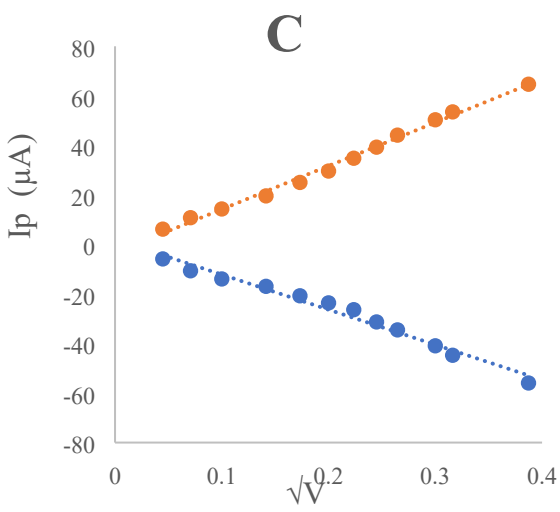
C
Ip (μA)
80
60
40
20
0
-20
-40
-60
-80
0
0.1
0.2
0.3
0.4
√V

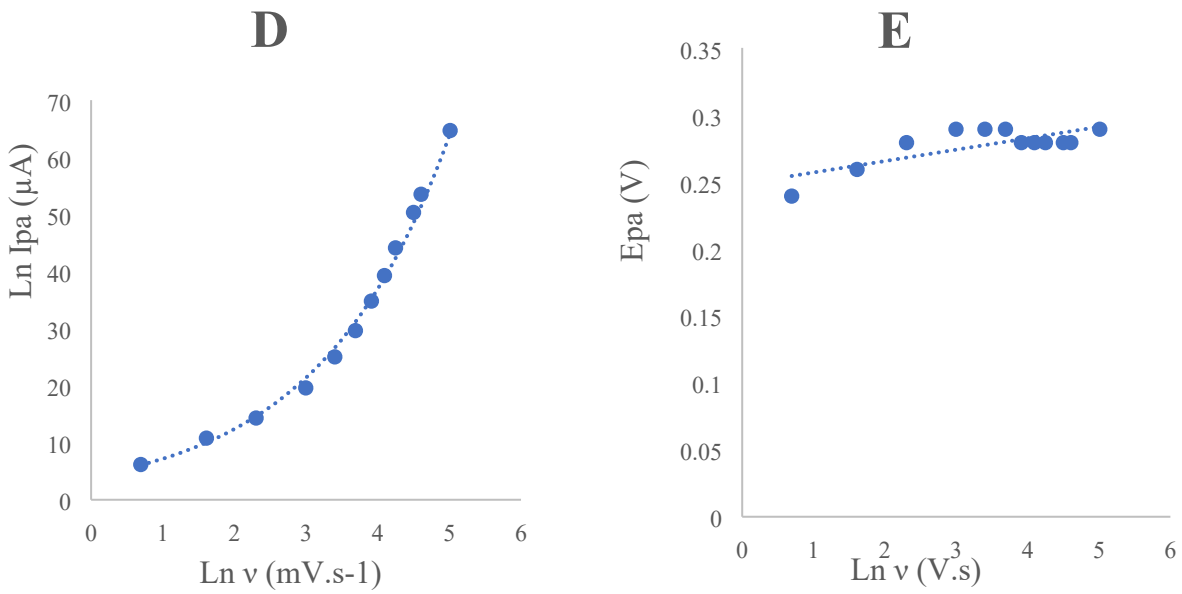

Fig. S10: A) CVs of GCE/P(CS)/KCC-1-nPr-NH-Arg/AgNPs in the process of $[Fe(CN)_6]^{3-/4-}$ solution in diverse sweep rates (0.15, 0.1, 0.09, 0.07, 0.06, 0.05, 0.04, 0.03, 0.02, 0.01, 0.005, 0.002 mV/s); **B)** Variation of I_p vs. v; **C)** Variation of I_p vs $v^{0.5}$; **D)** Variation of I_p vs. ln$v$; **E)** the plot of Napierian logarithm of oxidation peak current vs Napierian logarithm of sweep rates.